BULLETIN OF THE CHEMICAL SOCIETY OF JAPAN VOL. 43 1056—1061 (1970)

Optimum Geometric Position for Radioactivation by Fast Neutron with a Neutron Generator

Toshiaki KISHIKAWA and Chiro SHINOMIYA

Department of Industrial Chemistry, Faculty of Engineering, Kumamoto University, Kurokami-cho, Kumamoto

(Received June 19, 1969)

With a 14 MeV neutrol generator the optimum irradiation position of disk or square samples of appropriate numbers are given as a function of the configuration of the sample relative to the source. Calculated values are compared with experimental data.

In working with a 14 MeV neutron generator, the need arose to irradiate simultaneously several samples at the same flux. When only one sample is irradiated, the position nearest the deuteron beam spot provides the highest neutron flux.[1,2] When several samples are irradiated, the optimum irradiation position should be chosen at which the neutron flux gives the maximum value, and the radioactivation reaction gives the highest induced activity.

In a previous paper[1] geometry of irradiation was derived and calculated as a function of a generator-sample configuration. The calculated values were compared with the measured values of relative neutron flux. The geometry of irradiation is essentially the same as the geometry of radioactivity measurement. Extensive calculation of solid angles has been carried out.[3-9]

In this paper we report the optimum irradiation position of plane samples as a function of generator-sample configuration. Calculated values are compared with experimental data.

Theoretical

The following assumptions are made:

1. The shape of the neutron source is a point or a disk, emitting neutrons which are distributed uniformly throughout the source.
2. Mono-energetic neutrons (14 MeV) are emitted isotropically.
3. Thermalization and absorption by target holder, water cooling cap and air are neglected.

Geometry of Irradiation and Its Calculation. Neutron flux is different in various irradiation configuration. The flux to be measured is proportional to the numbers of neutron passing through the sample. The fraction of the flux ϕ in n/cm^2-sec to the neutron output N in n/sec is equal to the relative solid angle $\Omega/4\pi$ subtended by the sample. This is defined as the geometry G of irradiation corresponding to the geometry of instruments to measure radioactivity.

$$G = \phi/N = \Omega/4\pi \tag{1}$$

The solid angle Ω_P at a point source P subtended by the sample is given by

$$\Omega_P = \int_A \cos\gamma \frac{dA}{r^2} \tag{2}$$

1) C. Shinomiya and T. Kishikawa, *Tech. Repts. Kumamoto Univ.*, **16**, 68 (1968).
2) P. E. Wilkniss and G. J. Wynne, *Int. J. Appl. Radiat. Isotopes*, **18**, 77 (1967).
3) A. K. Kovarik and N. I. Adams, Jr., *Phys. Rev.*, **40**, 718 (1932).
4) B. P. Buritt, *Nucleonics*, **5**, 28 (1949).
5) M. Calvin, C. Heidelberger, J. C. Reid, B. M. Tolbert and P. Y. Yankwich, "Isotopic Carbon," John Wiley & Sons, New York (1949) p. 304.
6) A. H. Jaffey, *Rev. Sci. Instr.*, **25**, 349 (1954).
7) A. V. H. Masket, R. L. Macklin and H. W. Schmitt, ORNL-2170 (1956).
8) A. V. H. Masket, *Rev. Sci. Instr.*, **28**, 191 (1957).
9) F. Paxton, *ibid.*, **30**, 254 (1959).

TABLE 1. TYPICAL CLASSIFICATION OF GEOMETRY CALCULATION

Sample form	Source	Distance from Axis[a)]	Calculation		Ref.
			Equation	Solution	
Disk	Point	On axis	5	Given	5
Disk	Point	Off axis	6	Numerically integrated	
Square	Point	On axis	8	Solved	
Square	Point	Off axis	10	Solved	
Disk	Spread	On axis	11	Numerically integrated	
Disk	Spread	Off axis			1
Square	Spread	On axis			1
Square	Spread	Off axis			1

a) The expression "axis" means the direction which passes through a point or the center of a spread source, and which is normal to sample plane (see Fig. 1).

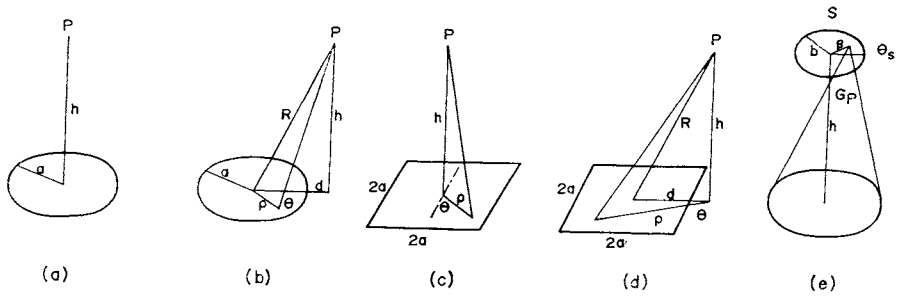

Fig. 1. Typical assemblies of source (point P or spread S) and a sample.

where

A = surface bounded by the sample.
r = distance from the source to a point Q on the sample.
γ = angle between the normal to the surface element dA at Q and the line PQ.

Substituting Eq. (2) into Eq. (1), we obtain

$$G_P = \frac{1}{4\pi}\int_A \cos\gamma \frac{dA}{r^2} \tag{3}$$

If the area of the source is too large to be approximated by a point, the average value of the geometry G_S of a spread source may be calculated by the equation[6)]

$$G_S = \frac{1}{N_S}\int_S G_P N_P dS \tag{4}$$

where

S = surface bounbed by neutron generation.
N_P = relative neutron output at a point P.
N_S = total neutron output.
G_P = geometry at a point P (Eq. 3).

It is possible only in a few cases to carry out the integration analytically where the symmetry of the configuration simplifies the calculation.

Geometry equations were derived for disk and square as functions of the generator-sample configuration in orthogonal coordinates. Typical classification of the geometry calculation is given in Table 1. The schematic configuration and summary of symbol definitions are given in Fig. 1.

The results of the derivation are as follows. Results which cannot be evaluated in closed form are expressed in integral forms.

A. Geometry of a point source coaxial with a disk (Fig. 1a) is derived by means of solid geometry elsewhere[5)]

$$G_P = \tfrac{1}{2}\left\{1 - \frac{h}{(a^2+h^2)^{1/2}}\right\} \tag{5}$$

B. Geometry in which the normal to the center of the disk does not pass the point source (Fig. 1b), is found to be

$$G_P = \frac{1}{4\pi}\int_0^a\int_0^{2\pi} \frac{\rho h d\rho d\theta}{(d^2+\rho^2+h^2-2d\rho\cos\theta)^{3/2}}$$

or

$$G_P = \frac{h}{2\pi}\int_0^{\pi} d\theta \left\{ \frac{ad\cos\theta + R^2}{(d^2\cos^2\theta - R^2)(R^2+a^2-2ad\cos\theta)^{1/2}} - \frac{R}{d^2\cos^2\theta - R^2} \right\} \tag{6}$$

where

$$R^2 = d^2 + h^2$$

If the sample is on the axis of the source, *i.e.* d is 0 in Eq. (6), then Eq. (6) can be reduced to Eq. (5).

C. Geometry of a point source coaxial with the

square (Fig. 1c) is given by

$$G_P = \frac{2}{\pi}\int_0^{a\sec\theta}\int_0^{\pi/4}\frac{\rho h\,d\rho\,d\theta}{(\rho^2+h^2)^{3/2}} \tag{7}$$

Equation (7) is then reduced to

$$G_P = \frac{1}{2} - \frac{2}{\pi}\sin^{-1}\frac{h}{(2a^2+2h^2)^{1/2}} \tag{8}$$

D. Geometry in which the normal to the center of the square dose not pass the point source (Fig. 1d) is found to be

$$G_P = \frac{1}{2\pi}\left[\int_{(d-a)\sec\theta}^{(d+a)\sec\theta}\int_0^{\tan^{-1}a/(d+a)}\frac{\rho h\,d\rho\,d\theta}{(\rho^2+h^2)^{3/2}} + \int_{(d-a)\sec\theta}^{a\operatorname{cosec}\theta}\int_{\tan^{-1}a/(d-a)}^{\tan^{-1}a/(d+a)}\frac{\rho h\,d\rho\,d\theta}{(\rho^2+h^2)^{3/2}}\right] \tag{9}$$

Equation (9) is then reduced to

$$G_P = \frac{1}{2\pi}\left[\sin^{-1}\frac{ah}{\{(d-a)^2+h^2\}^{1/2}\{(d-a)^2+a^2\}^{1/2}} - \sin^{-1}\frac{ah}{\{(d+a)^2+h^2\}^{1/2}\{(d+a)^2+a^2\}^{1/2}} + \sin^{-1}\frac{(d-a)h}{(a^2+h^2)^{1/2}\{(d-a)^2+a^2\}^{1/2}} - \sin^{-1}\frac{(d+a)h}{(a^2+h^2)^{1/2}\{(d+a)^2+a^2\}^{1/2}}\right] \tag{10}$$

E. Geometry of a spread source coaxial with a disk (Fig. 1e) is given from Eqs. (4) and (6) by replacing d with β in Eq. (6). We have

$$G_S = \frac{2}{b^2}\int_0^b \beta G_P(\beta)\,d\beta$$

or

$$G_S = \frac{h}{\pi b^2}\int_0^b\int_0^\pi \beta\,d\beta\,d\theta_S \times\left[\frac{\beta^2+h^2-2a\beta\cos\theta_S}{\{\beta^2\cos^2\theta_S-(\beta^2+h^2)\}\{a^2+\beta^2+h^2-2a\beta\cos\theta_S\}^{1/2}} - \frac{(\beta^2+h^2)^{1/2}}{\beta^2\cos^2\theta_S-(\beta^2+h^2)}\right] \tag{11}$$

Numerical data of the derivations A—E and a summary of the geometry (F) in which the normal to the center of the disk does not pass the center of the source, (G) in which the normal to the center of the square passes the center of the source, and

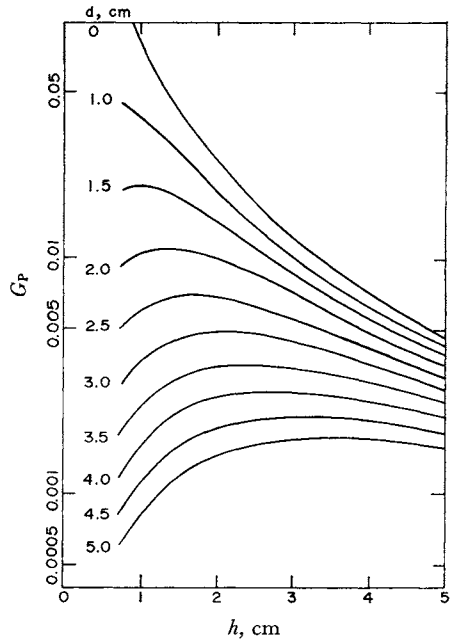

Fig. 2. Geometry value G_P of a point source of a disk (radius 0.665 cm). The G_P curve is given for each distance from axis d.

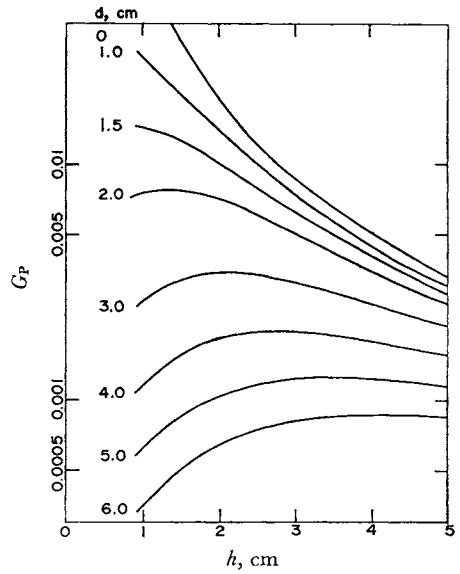

Fig. 3. Geometry value G_P of a point source of a square (side 1 cm). The G_P curve is given for each distance from axis d.

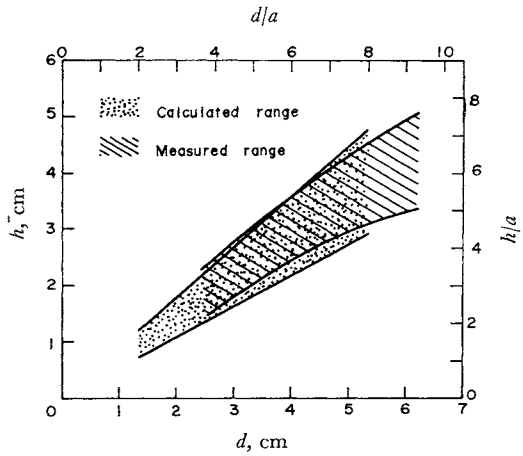

Fig. 4. The optimum geometric position of 97% confidence range of a disk sample with a radius of a=0.665 cm or with an unit radius.

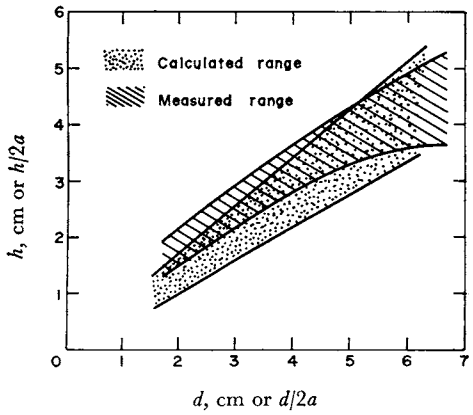

Fig. 5. The optimum geometric position of 97% confidence range of a square sample with a side of $2a=1$ cm or with an unit side.

(H) in which the normal to the center of the square dose not pass the center of the source, have been reported.[1)]

For disk (radius $a=0.665$ cm) and square (side $2a=1$ cm) the geometry values of the series A—D are numerically integrated and shown in Figs. 2 and 3.

The optimum geometry with respect to h can be given analytically by solving the equation $(\partial G/\partial h)_{a,b,d}=0$. This was obtained graphically in Figs. 2 and 3. The optimum geometric position of 97% confidence range in (d, h) with a radius of $a=0.665$ cm or with a side of $2a=1$ cm, so obtained, are shown in Figs. 4 and 5.

Experimental

Neutron Generator. Monochromatic 14 MeV neutrons were produced by $^{3}H(d, n)^{4}He$ reaction with a vertical-type neutron generator made by Hitachi Ltd. A thin tritiated titanium target (*ca.* 5 Ci; copper based) was bombarded with a deuteron beam of *ca.* 200 μA and *ca.* 100 kV. The neutron output was kept constant by controlling the accelerating voltage of the generator. The output was recorded by a BF_3 counter with a counting-rate meter.

Determination of Deuteron Beam Position. It was important to keep the position of deuteron beam spot, or the center of the neutron emission constant. The determination was made by irradiating a small copper foil. The foils ($5\times5\times0.5$ mm) were placed square or crosswise on the cooling cap in the plane parallel to the tritiated target. From the distribution of the induced activity of the foils, the center of the neutron emission was determined by plotting the activity *versus* position. Typical examples are shown in Figs. 6a and 6b.

In the case of the squares method, a contour map (see Fig. 6a) was obtained. The limited numbers of the foil made it difficult to draw a contour of an appropriate level of activity. In the case of the cross method, the plot of activity against position axes gave bloken lines. The ordinates of the folds showed the center (see Fig. 6b). The method was found to be useful.

Determination of Irradiation Geometry. Variation of neutron flux at the irradiation position with respect to the generator-sample configuration was determined by measuring the induced activity of the sample. Copper foil was chosen as a sample. It was a disk (radius 0.665 cm) or a square (side 1 cm).

In order to determine flux at a particular position,

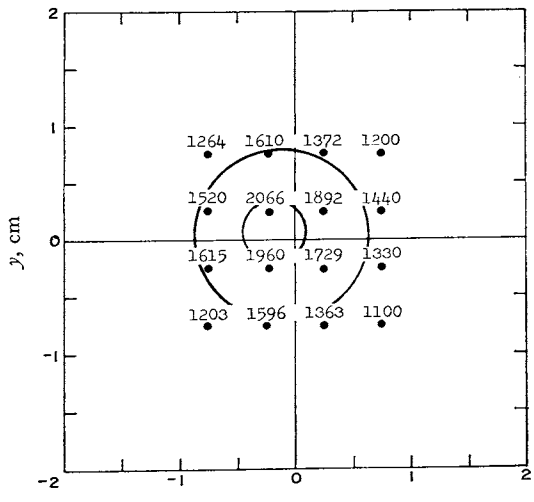

(a) Squares method; center $(-0.2_0, 0.0_6)$

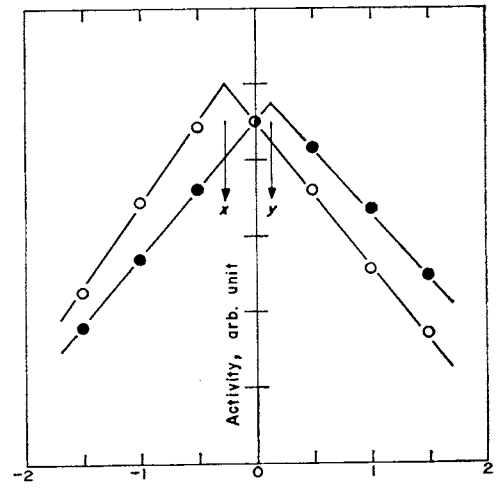

(b) Cross method; center $(-0.2_5, 0.1_3)$

Fig. 6. Determination of the center of the deuteron beam spot, or the center of neutron emission by activating copper foils. In the figure (a) activity values in cpm are superimposed. Contours are 1500 and 2000 cpm level.

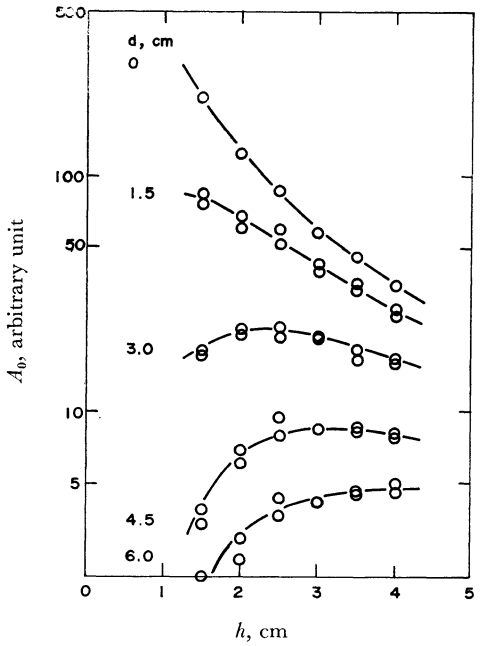

Fig. 7. Induced activity values of disk samples. The radius is 0.665 cm.

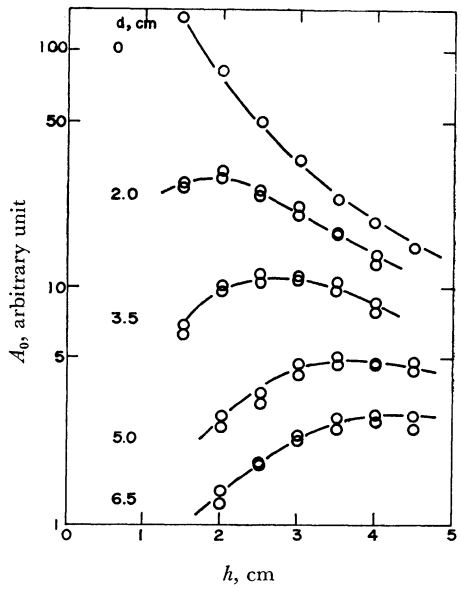

Fig. 8. Induced activity values of square samples. The side is 1 cm.

TABLE 2. RATIO OF INDUCED ACTIVITY TO GEOMETRY OF SPREAD SOURCE COAXIAL WITH A DISK SAMPLE

Axial distance h, cm	Induced activity A_0, cpm	A_0/G_S values $\times 10^{-5}$ at b in cm					
		0[a]	0.1	0.2	0.3	0.4	0.5
1.5	22200	5.12	5.19	5.22	5.29	5.38	5.49
2.0	13600	5.33	5.33	5.36	5.40	5.46	5.53
2.5	8820	5.25	5.26	5.27	5.30	5.34	5.39
3.0	6310	5.33	5.33	5.34	5.36	5.39	5.43
3.5	4550	5.12	5.18	5.19	5.20	5.23	5.25
	average	5.230	5.258	5.276	5.310	5.310	5.418
	S. D., %	1.807	1.235	1.249	1.294	1.707	1.926

a) Point source, A_0/G_P values.

the foils were placed normal to the direction of deuteron beam and irradiated for several minutes. In order to give uniform neutron emission to the foils, they were rotated with the sample mounting. The induced activity of each foil was then measured in turn to follow its decay with an end-window G-M counter. The decay curve showed the presence of ^{62}Cu (half-life 9.8 min). Possible influence of ^{66}Cu (half-life 5.1 min) produced from ^{65}Cu$(n, \gamma)^{66}$Cu reaction and the other nuclides (^{64}Cu and ^{65}Ni) produced from the fast neutron activation could be neglected. Counting rates of the individual samples were corrected for slight weight differences. All the samples were not irradiated at the same time. A comparator technique was used to correlate separate irradiation at different output levels.

The relation between induced activity A_0 at the end of irradiation and flux ϕ can be given by

$$A_0 = N_0\phi\sigma(1-e^{-\lambda t}) \qquad (12)$$

When a foil with known N_0 is irradiated for a certain time t, the term $N_0\sigma(1-e^{-\lambda t})$ in Eq. (12) remains constant. Thus the induced activity is proportional to the neutron flux at the irradiation position or the irradiation geometry. The results are shown in Figs. 7 and 8.

Size of Deuteron Beam Spot. If samples along the direction of the deuteron beam are irradiated (radius of the focus b in cm), the ratio of induced activity to geometry $A_0(h)/G_S(h)$ may remain constant independent of the irradiation distance h. The calculated ratio with the values of $G_S(h)$ given previously[1] at appropreate values of b are listed in Table 2. In the case that b is 0.0, the ratio is equal to $A_0(h)/G_P(h)$. If the value of b is equal to the radius of the neutron emitting spot at which the percent standard deviation of the values of $A_0(h)/G_S(h)$ is minimized, the radius of *ca.* 0.1 cm can be obtained.

The actual size of the focus of the deuteron beam can be seen directly by replacing the tritiated target with a quartz plate. Induced fluorescence showed an

ellipse-like figure, whose diameters are found to be *ca.* 3 mm and *ca.* 5 mm. Its color showed non-uniform intensity. With quartz plate the calculated value was smaller than the observed value. It is probably because (1) the neurton emission is assumed to be distributed unformly throughout the beam spot, and (2) the shape of the spot is assumed to be a disk.

Optimum Irradiation Geometry. The observed values of induced activity at various distances d against distance h shown in Figs. 7 and 8 indicate the presence of maximum values of A_0 and that at d is zero. The experimentally obtained optimum position of 97% confidence range expressed in the coordinates (d, h) which can be found in Figs. 7 and 8 are shown in Figs. 4 and 5. The ranges obtained are in fairly good agreement with the theoretically derived ranges which are shown in the same figures.

As the value of geometry is only a function of the source-sample configuration, the ratio $a : d : h$ is constant. (If the radius of a disk is greater than or equal to 0.665 cm, the value of $G_S(h)$ becomes nearly equal to the value of $G_P(h)$ for $h=1.5$ cm.[1]) This indicates that it is sufficient, under the appropriate empirical conditions, to assume the beam focus to be a point.) This leads to the homologous relation. If the value of a is set up, an optimum position (d, h) is found in scale of d/a and h/a respectively in Fig. 4 or 5. If definite numbers n of disk or square sample (appropreate size a) are irradiated simultaneously under the same neutron flux, the optimum distance d from the axis can be found by means of the relation

$$d = a\mathrm{cosec}\pi/n \quad \text{for disk} \tag{13}$$

or

$$d = a(1+\cot\pi/n) \quad \text{for square} \tag{14}$$

Hence the optimum configuration can be obtained in Fig. 4 or 5.

As the capsule used for the irradiation of powder or liquid is cylindrical, and the optimum range of irradiation geometry is fairly wide, the present data can be utilized for the choice of the generator-cylindrical sample configuration.

The authors wish to express their gratitude to Dr. Shoichi Sato, Dept. of Mathematics, for his advice and encouragement, and to Professor Kimikazu Matsuyama, Dept. of Electrical Engineering, Chief of the Computing Center, for providing facilities of FACOM-231 computer and for his help with programming. Thanks are also due to Mr. Masaya Tanizaki for the operation of the neutron generator.